3. Soot primary particle nucleation rates in laminar premixed and diffusion flames were similar for comparable temperatures and concentrations of H and acetylene. A crude correlation of soot primary particle nucleation rates was achieved using these variables but a more complete model of soot nucleation that accounts for soot precursor species and processes of coalescence, dehydrogenation, etc., should be sought in order to achieve a more complete and robust treatment of soot nucleation.

(3) /cw/in/25

4. Laminar Diffusion Flame Studies (Ground- and Space-Based Studies)

4.1 Introduction

Laminar diffusion flames are of interest because they provide model flame systems that are far more tractable for analysis and experiments than more practical turbulent diffusion flames. Certainly, understanding flame processes within laminar diffusion flames must precede understanding these processes in more complex turbulent diffusion flames. In addition, many properties of laminar diffusion flames are directly relevant to turbulent diffusion flames using laminar flamelet concepts. Laminar jet diffusion flame shapes (luminous flame boundaries) have been of particular interest since the classical study of Burke and Schumann (1928) because they are a simple nonintrusive measurement that is convenient for evaluating flame structure predictions. Thus, consideration of laminar flame shapes is undertaken in the following, emphasizing conditions where effects of gravity are small, due to the importance of such conditions to practical applications.

Another class of interesting properties of laminar diffusion flames are their laminar soot and smoke point properties (i.e., the flame length, fuel flow rate, characteristic residence time, etc., at the onset of soot appearance in the flame (the soot point) and the onset of soot emissions from the flame (the smoke point)). These are useful observable soot properties of nonpremixed flames because they provide a convenient means to rate several aspects of flame sooting properties: the relative propensity of various fuels to produce soot in flames; the relative effects of fuel structure, fuel dilution, flame temperature and ambient pressure on the soot appearance and emission properties of flames; the relative levels of continuum radiation from soot in flames; and effects of the intrusion of gravity (or buoyant motion) on emissions of soot from flames. An important motivation to define conditions for soot emissions is that observations of laminar jet diffusion flames in critical environments, e.g., space shuttle and space station facilities, cannot involve soot emitting flames in order to ensure that test chamber windows used for experimental observations are not blocked by soot deposits, thereby compromising unusually valuable experimental results. Another important motivation to define conditions where soot is present in diffusion flames is that flame chemistry, transport and radiation properties are vastly simplified

when soot is absent, making such flames far more tractable for detailed numerical simulations than corresponding soot-containing flames.

Motivated by these observations, the objectives of this phase of the investigation were as follows:

1. Observe flame-sheet shapes (the location of the reaction zone near ϕ=1) of nonluminous (soot free) laminar jet diffusion flames in both still and coflowing air and use these results to develop simplified models of flame-sheet shapes for these conditions.

2. Observe luminous flame boundaries of luminous (soot-containing) laminar jet diffusion flames in both still and coflowing air and use these results to develop simplified models of luminous flame boundaries for these conditions. In order to fix ideas here, maximum luminous flame boundaries at the laminar smoke point conditions were sought, i.e., luminous flame boundaries at the laminar smoke point.

3. Observe effects of coflow on laminar soot- and smoke-point conditions because coflow has been proposed as a means to control soot emissions and minimize the presence of soot in diffusion flames, see Dai and Faeth (2000) and Lin and Faeth (1996a,1996b).

The following description of this phase of the research is relatively brief. Additional details may be found in Dai and Faeth (2000), Lin and Faeth (1996a,1996b,1998,1999,2000), Lin et al. (1999), Urban et al. (1998,2000) and Xu et al. (2000b).

4.2 Experimental Methods

Flames in Still Air. Two flame conditions were considered, involving laminar jet diffusion flames in still and coflowing air. Present interests were devoted to nonbuoyant flames which was achieved either by carrying out experiments using ground-based (drop tower, aircraft) or space-based (space shuttle) microgravity facilities or by carrying out experiments at normal gravity but at reduced pressures which provides a way of simulating small gravity conditions as discussed by Law and Faeth (1994). Finally measurements at normal gravity but at reduced pressures with strong coflow also involve conditions where effects of buoyancy are small (Dai and Faeth, 2000).

Several test arrangements were used for laminar jet diffusion flames in still air but they were all similar to the space shuttle facility used by Lin et al. (1999) and Urban et al. (1998,2000). In this facility, laminar jet diffusion flames were stabilized at the exit of round fuel

nozzles located along the axis of a windowed chamber. The chamber had a diameter of 400 mm and a maximum length of 740 mm and was operated at pressures of 35-130 kPa in air environments. Various round fuel nozzles were used having thin tube walls. The nozzle inlets had flow straighteners and length/diameter ratios greater than 55:1 to yield fully developed laminar pipe flow at the nozzle exit.

Monitoring measurements included fuel flow rates, fuel temperature, chamber pressure and chamber temperature. Flame shapes were measured using a color video camera (Hitachi Model KP-C553) with a spatial resolution better than 0.3 mm. Photographs were also obtained using a filter designed to pass radiation from the excited CH band associated with radical reactions in the flame sheet (430 nm center frequency with 10 nm half-width pass band), which provided a way to find the flame sheet in the presence of luminous yellow soot luminosity.

Original sources should be consulted to find detailed information about test conditions. The main test parameters were as follows: fuels included methane, acetylene, ethylene, propylene, propane and 1-3 butadiene; burner diameters were 0.8-5.4 mm; burner exit Reynolds numbers were 2-172, luminous flame lengths were 5-108 mm and pressures were 3-100 kPa.

Flames in Coflowing Air. Detailed descriptions of this facility can be found in Lin et al. (1996a), Dai and Faeth (2000), and Xu et al. (2000b). The burner was placed in a cylindrical chamber, directed vertically upward, with the tests generally carried out at pressures smaller than 50 kPa in order to minimize effects of buoyancy. The burner was a coaxial-tube arrangement with the fuel flowing from the inner port and air flowing from a concentric outer port (60-mm inside diameter). The inner port had sufficient length to yield fully developed laminar pipe flow at the burner exit. Flame lengths were limited so that test conditions approximated flames in a uniform air coflow. The windowed chamber had a diameter of 300 mm and a length of 1200 mm. Optical access was provided by pairs of opposing windows having diameters of 100 mm.

Monitoring measurements were the same as for flames in still air, except that the air coflow velocity was monitored as well. In this case, flame shapes were obtained using a 35 mm reflex camera, subsequently printing the photographs using a 100×125 mm film format. The flame shapes were measured directly from the films.

Original sources should be consulted to find detailed information about test conditions. The main test parameters were as follows: fuels included methane, acetylene, ethylene, propylene, propane, and 1-3 butadiene; fuel port diameters were 1.6-6.0 mm; burner exit Reynolds numbers were 2-219; ratios of initial air/fuel velocities were 0.008-32.5; luminous flame lengths were 5-108 mm; and pressures were 3.5-50 kPa.

4.3 Theoretical Methods

Flames in Still Air. The goal of analysis was to develop a convenient way of interpreting and correlating the flame shape measurements. A set of easily used equations was sought, along with recommendations for selecting the thermodynamic and transport properties appearing in these equations, as opposed to more complete methods that would require numerical solutions on a computer. Two conditions were considered; namely, laminar jet diffusion flames in still air and in coflowing air at nonbuoyant conditions.

The basis of the analysis of nonbuoyant laminar jet diffusion flames in still air was the simplified analysis of Spalding (1975). The major assumptions of this analysis are as follows: (1) only steady, axisymmetric laminar jet diffusion flames at constant pressure in still environments are considered; (2) effects of buoyancy and potential energy changes are small; (3) the Mach number of the flow is small so that effects of viscous dissipation and kinetic energy changes can be ignored; (4) the flame has a large aspect ratio so that diffusion of mass (species), momentum and energy in the streamwise direction is small; (5) for the same reasons, the solution of the governing equations can be approximated by far-field conditions where the details of initial conditions at the jet exit can be replaced by jet invariants for the conservation of mass (elements), momentum and energy in the integral sense; (6) all chemical reactions occur in a thin flame sheet with fast chemistry so that fuel and oxidant are never simultaneously present within the flame; (7) the diffusivities of mass (of all species), momentum and energy are all equal; (8) all thermophysical and transport properties are constant throughout the flame; and (9) effects of radiation are small. The assumptions are discussed by Lin et al. (1999). The last three, however, are not satisfied by laminar diffusion flames and are only adopted so that simple formulas for flame shape can be found, and due to the past success of similar approximations for analysis of the shapes of laminar diffusion flames (Spalding, 1975).

The formulas for flame shapes obtained using these approximations appear in Lin et al. (1999). Correlation of these formulas with measurements was sought by selecting conditions to find mean transport parameters and introducing some empirical parameters, as follows: the equal diffusivity approximation was replaced by introducing the Schmidt number, $Sc = 0.76$, based on air properties; transport properties were taken to be the properties of air at the average of the adiabatic flame temperature and the ambient temperature; the correlations were extended to small aspect ratios by introducing a virtual origin, L_o; and an empirical coefficient, C_f, was introduced to best fit the correlations to measurements and account for effects of differences between soot and flame sheet luminosity. With these changes, the luminous flame length becomes:

$$(L_f-L_o)/d = (3C_f/32)ReSc/Z_{st} \quad (12)$$

whereas, the expression for the luminous flame diameter becomes:

$$wZ_{st}/d = 3^{1/2}\zeta(\zeta^{-1/2} - 1)^{1/2} \quad (13)$$

where

$$\zeta = (z-L_o)/(L_f-L_o) \quad (14)$$

Flames in Coflowing Air. The basis for the analysis of nonbuoyant laminar jet diffusion flames in coflowing air was the same as Lin et al. (1999) for flames in still air, and the assumptions used in the analysis were the same as well. The resulting equation for the luminous flame length becomes:

$$(L_f-L_o)/d = (C_f/16)ReSc/Z_{st} \quad (15)$$

whereas, the expression for the luminous flame diameter becomes:

$$wZ_{st}/d = [-\zeta(u_{fo}/u_{ao})Z_{st}\ln\{\zeta\}]^{1/2} \quad (16)$$

where ζ can be found from Eq. (14) as before. The algorithm for finding physical properties in Eqs. (15) and (16) was also the same as for the flames in still air. Remarkably, Eq. (15) indicates that luminous flame lengths in coflow are proportional to the mass flow rate of fuel and independent of coflow velocity, similar to flames in still air, but they are only 2/3 as long. Direct effects of coflow velocity also manifest themselves with respect to flame diameters, as is evident from Eq. (16).

4.4 Flame Shape Properties

Luminous Flame Lengths. Measured and predicted luminous flame lengths for nonbuoyant laminar jet diffusion flames in still air are illustrated in Fig. 14. These results are plotted according to Eq. (12) for tests carried out at microgravity using Space Shuttle facilities for ethylene- and propane-fueled flames burning in still air. These results involved soot-containing flames at the laminar smoke point where yellow soot luminosity extends significantly beyond the flame sheet where ϕ=1. Best fit values of the empirical parameters were $L_o/d = -3.2$ and $C_f = 1.13$. The simplified theory of Eq. (12) does a remarkably good job of correlating the

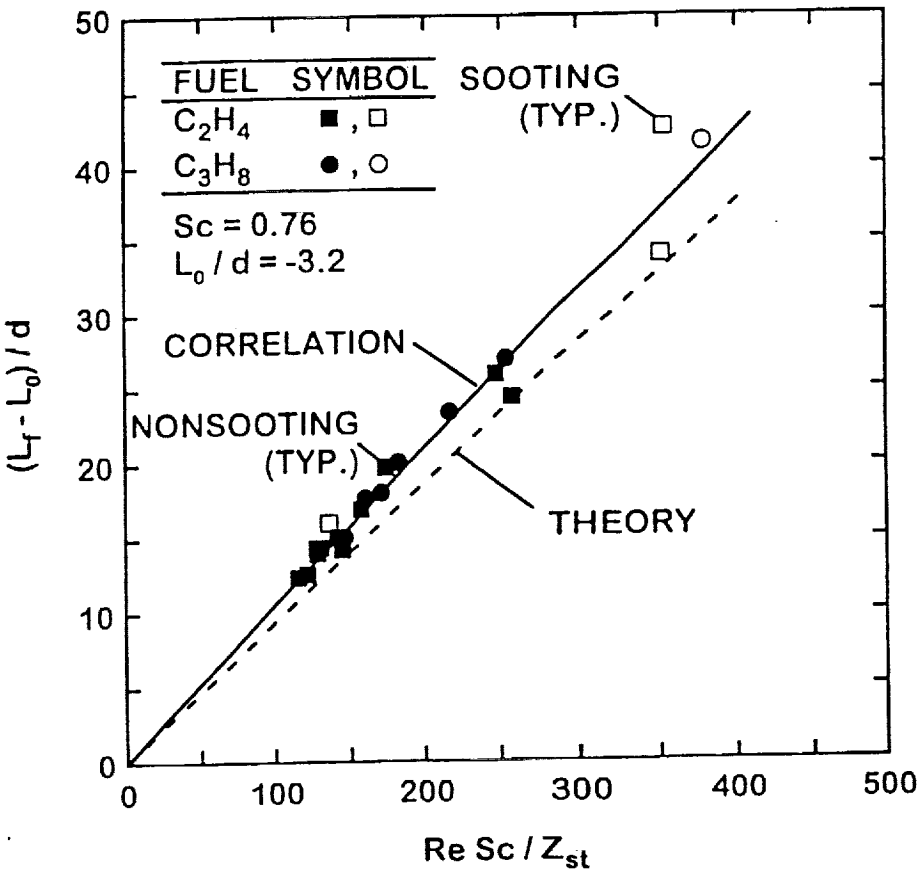

Fig. 14 Measured and predicted luminous flame lengths of nonbuoyant hydrocarbon/air laminar jet diffusion flames as a function of normalized jet exit Reynolds number. From Lin et al. (1999).

measurements with the baseline result, for C_f=1, very close to the measurements. Flame lengths at the laminar smoke point are also seen to be not much affected by whether or not the flames were actually emitting soot.

Several additional determinations of luminous flame lengths are plotted as suggested by Eq. (12) in Fig. 15 in order to gain insight about effects of unsteadiness, buoyancy and soot luminosity. All the measurements are correlated quite nicely according to Eq. (12) but values of C_f differ considerably. The results for low gravity tests using the KC-135 facility are closest to the space-based data but are significantly shorter with C_f=0.8 (e.g., the space-based flames are 40% longer) due to effects of disturbances to the gravitational field (g-jitter) with enhanced mixing due to these disturbances tending to reduce luminous flame lengths. The next closest results involved luminous flame lengths of soot-containing flames near the laminar smoke point at normal gravity yielding C_f=0.57 due to enhanced mixing resulting from buoyant motion. The last results are due to Sunderland et al. (1998) which yield luminous flame lengths very similar to the results for buoyant flames with C_f=0.56 but for very different reasons. These flames involved nonbuoyant soot-free (blue) methane, ethane- and propane-fueled flames burning in still air at microgravity conditions using a 2.2s drop tower facility. In this case, burner velocities, fuel flow rates and ambient pressures were manipulated to eliminate the presence of soot and enhance rates of flame development to steady conditions. Thus, it is likely that these results involve observations of the flame sheet itself whereas luminous flame lengths of soot-containing flames at the laminar smoke point involve yellow luminosity from soot that is present beyond the flame sheet and well into the fuel-lean region before the luminosity disappears when the soot finally burns out due to soot oxidation. Thus, for steady nonbuoyant laminar jet diffusion flames in still gases, luminous flame lengths at the laminar smoke point are roughly twice as long as the maximum streamwise position of the flame sheet due to soot luminosity in the fuel-lean region beyond the flame sheet.

As suggested by the equations for luminous flame lengths from the simplified theories, Eqs. (12) and (15), coflow also affects luminous flame lengths. This behavior is illustrated in Fig. 16 which involves measurements and correlations based on Eqs. (12) and (15), as follows: smoke-point flame lengths in still gases (C_f=1.05) from Lin et al. (1999); smoke-point flame lengths in coflow (C_f=1.05) from Lin and Faeth (1999), soot-point flame lengths in still gases (C_f=0.52) from Xu et al. (2000b) and soot-point flame lengths in coflow (C_f=0.54) from Xu et al. (2000b). It is evident that the flame length measurements for all these flows are correlated quite well by Eqs. (12) and (15). In particular, for similar soot conditions (soot-free or at the laminar smoke point) flames in still gases are roughly 50% longer than in still gases as prescribed by the simplified theories. In addition, values of C_f at the laminar smoke point condition are roughly twice as large as those for soot-free flames at comparable conditions; thus, the presence of hot

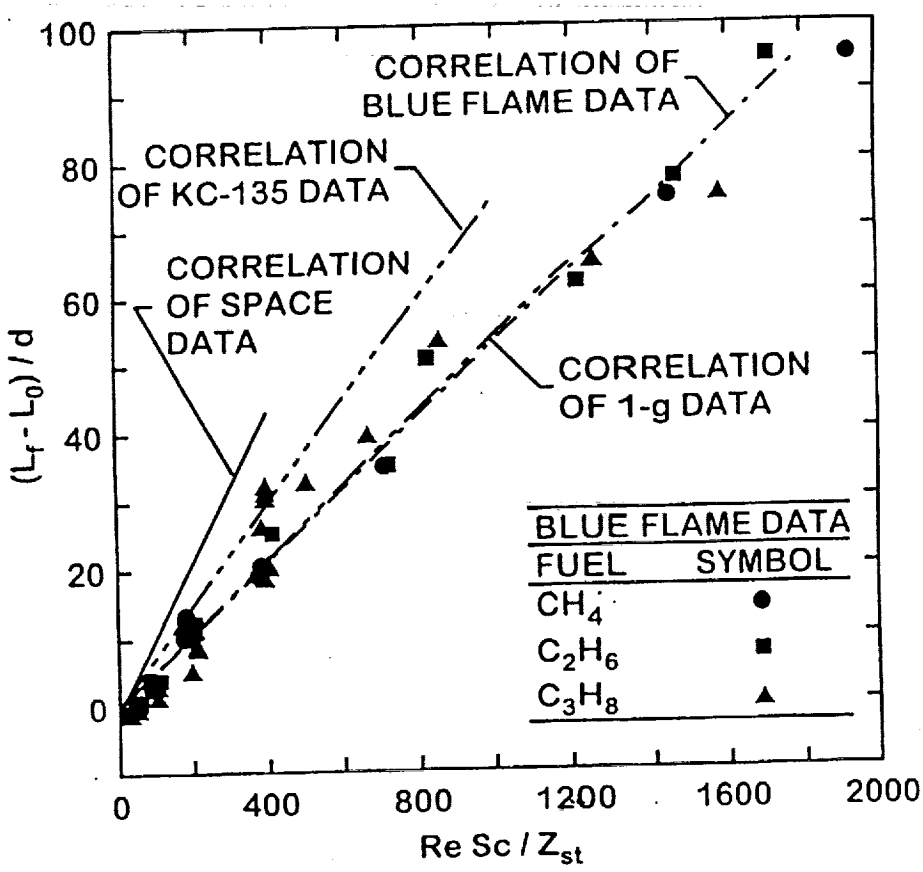

Fig. 15 Luminous flame lengths of hydrocarbon/air laminar jet diffusion flames as a function of normalized jet exit Reynolds number: correlation of measurements of soot-free (blue) flames from Sunderland et al. (1998), measurements (symbols) and correlation (line) of normal-gravity flames reported by Urban et al. (1999), and correlation of luminous nonbuoyant flame lengths from Urban et al. (1998). From Lin et al. (1999).

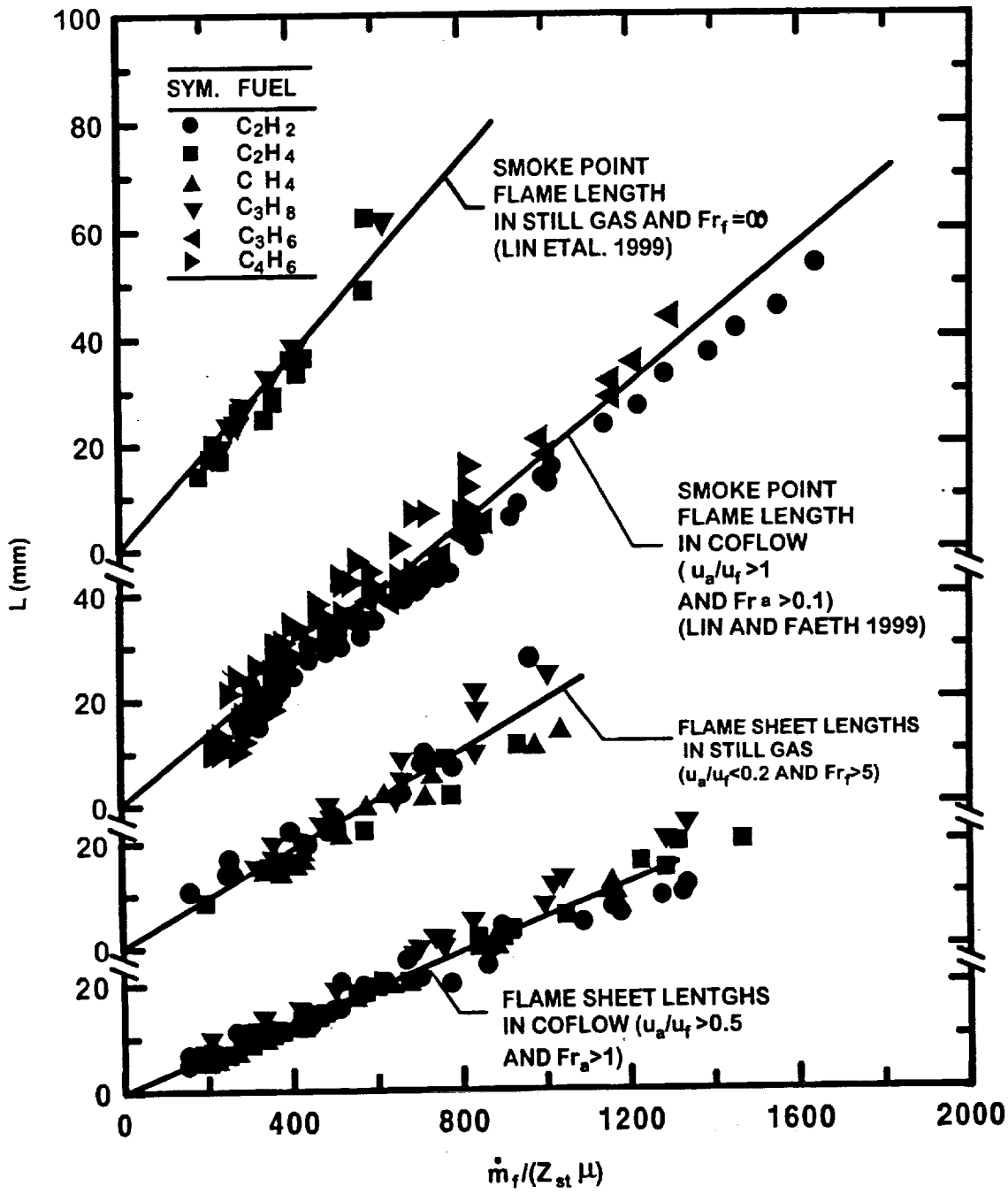

Fig. 16 Correlations between laminar soot and smoke-point flame lengths and normalized fuel flow rates for laminar jet diffusion flames in still and coflowing air for flames fueled with various hydrocarbons: smoke-point flame lengths in still gases from Lin et al. (1999), smoke-point flame lengths in coflow from Lin and Faeth (1999), soot-point flame lengths in still gases from Xu et al. (2000b), soot-point flame lengths in coflow from Xu et al. (2000b). Measurements (symbols) and predictions (lines). From Xu et al. (2000b).

soot particles in the fuel-lean portion of the flame significantly extends (by up to a factor of roughly 2) the region where flame luminosity is observed.

Luminous Flame Shapes. Measured and predicted flame shapes are illustrated in Fig. 17 for flames at the laminar smoke point in still gases, in Fig. 18 for flames at the laminar smoke point in coflowing gases, and in Fig. 19 for soot-free flames in coflowing gases. The last shows the results for flame sheet locations with and without the C-H filter, indicating that both methods provide good indications of the location of the flame sheet in this instance. The agreement between the flame shape measurements and the predictions of the simplified theories is remarkably good, which generally is the case when predicted flame lengths are accurate. The main exception is the near-injector condition in strong coflow where the assumptions of a large aspect ratio, boundary layer type of flow, are not valid and predictions are not expected to be accurate.

4.5 Soot and Smoke-Point Properties

Introduction. Several properties of soot-containing diffusion flames were of interest during the present investigation in addition to the flame structure, soot growth, soot oxidation, soot nucleation and flame shape properties that have already been discussed. The first of these relates to simplified ways to model the structure of practical soot-containing turbulent diffusion flames by exploiting well known methods using the laminar flamelet approximation which involves finding state relationships for scalar properties solely as a function of the degree of mixing of the flow, typically represented by the local mixture fraction of the flow. Such ideas have been considered for modeling turbulent diffusion flames since the early work of Hawthorne et al. (1949). Bilger (1976) demonstrated the existence of state relationships for the concentrations of major gas species even in soot-containing diffusion flames, leading to successful predictions of turbulent diffusion flame structure and radiation properties in some instances, see Gore and Faeth (1986,1988). Similar success was not achieved for soot properties in flames, however, due to the problems of buoyant laminar diffusion flames properly representing soot properties in turbulent diffusion flames (where local effects of buoyancy are small) that were discussed in connection with Fig. 1 (also see Faeth (2001) and Law and Faeth (1994)). Thus, one part of the present work sought better understanding of the potential for soot property state relationships in turbulent diffusion flames.

Several properties representative of the soot and smoke-point properties of laminar diffusion flames (defined as the laminar flame lengths at conditions where the flame just begins to emit and to contain soot, respectively) were also studied during the present investigation.

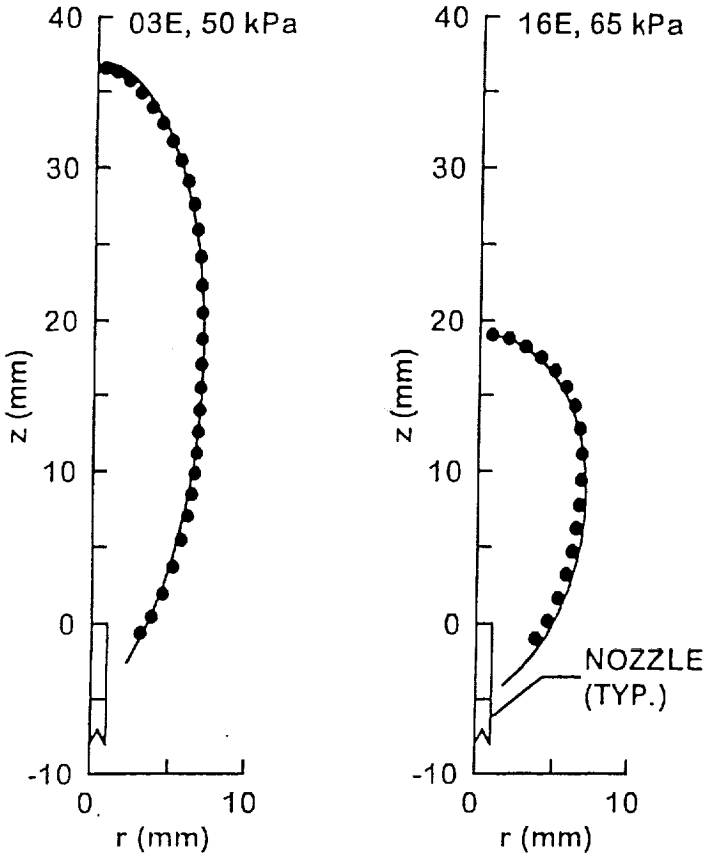

Fig. 17 Measured and predicted luminous flame shapes for typical closed-tip nonbuoyant hydrocarbon/air laminar jet diffusion flames in still air. From Lin et al. (1999).

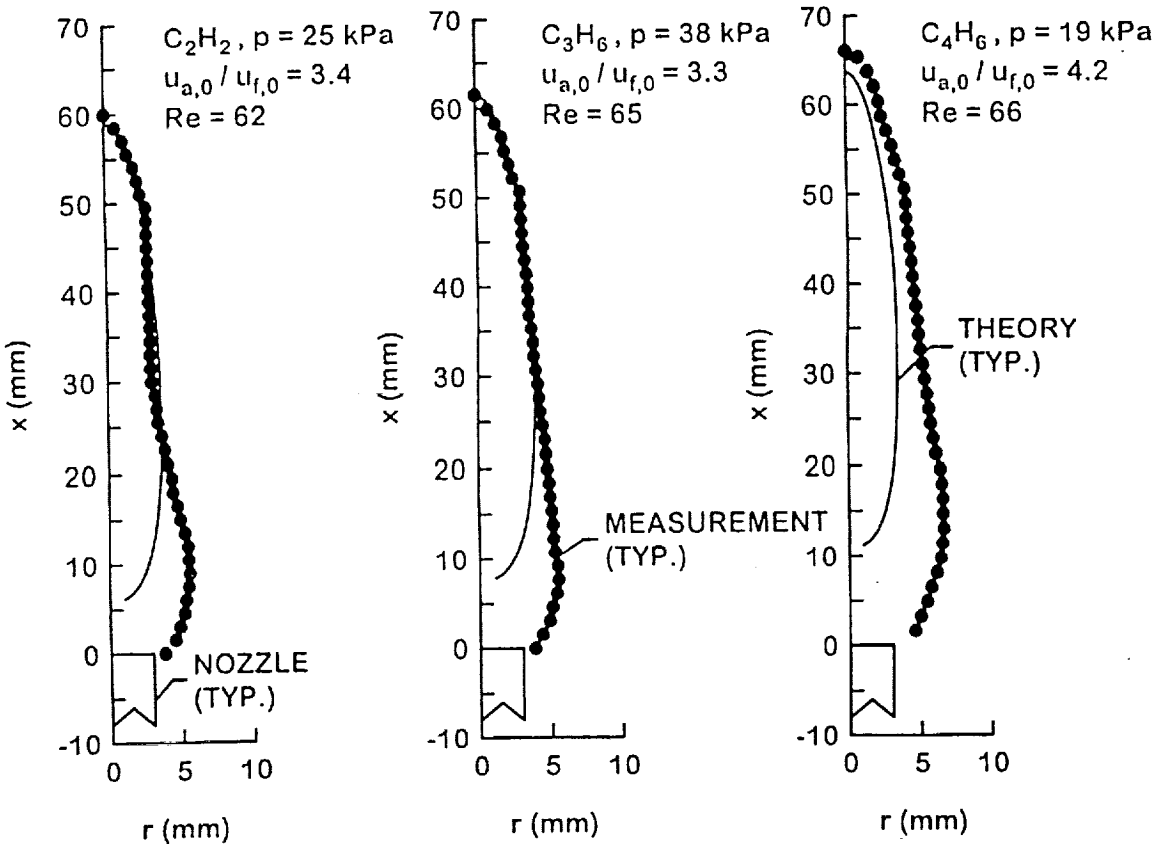

Fig. 18 Measured and predicted luminous flame shapes for typical hydrocarbon-fueled laminar jet diffusion flames in coflowing air. Lin and Faeth (1999).

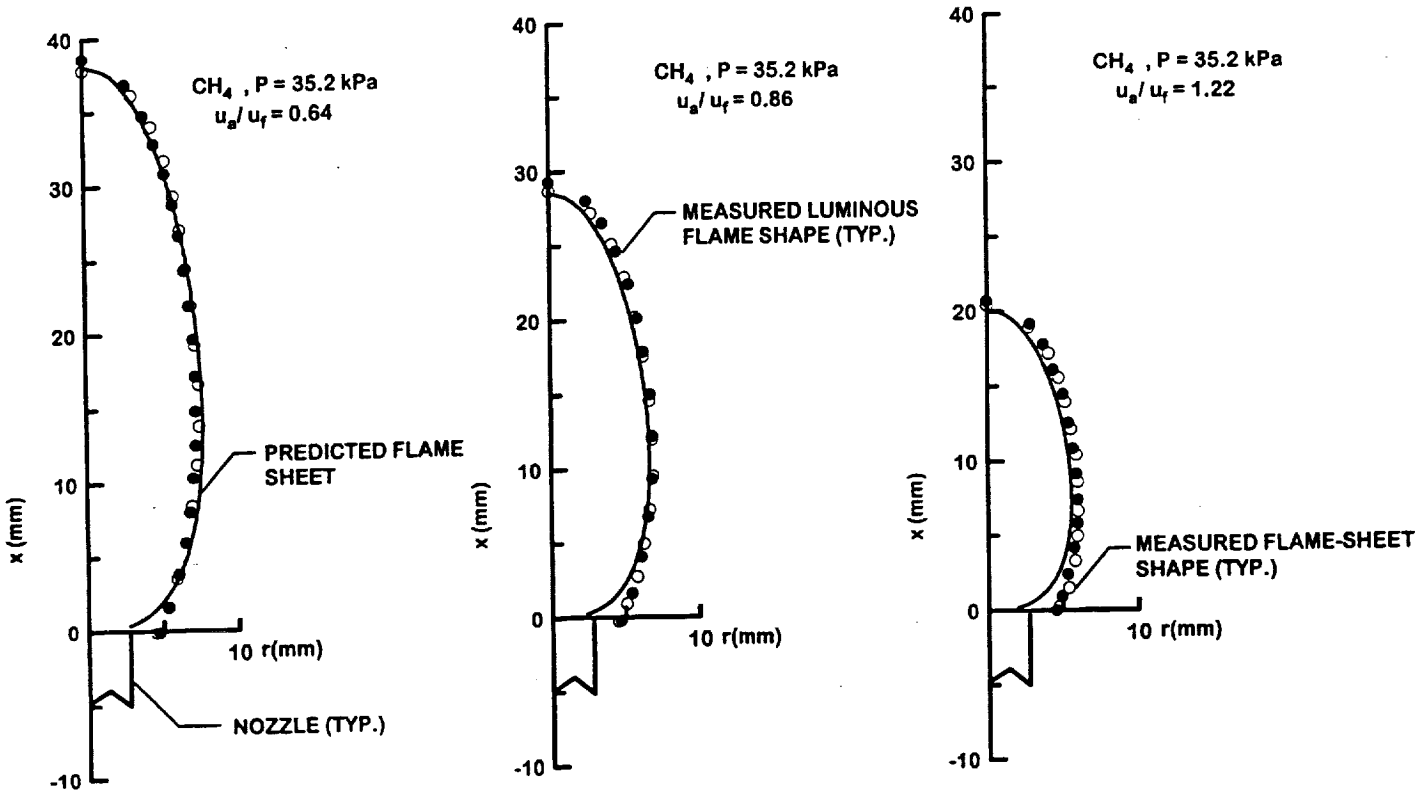

Fig. 19 Measured and predicted flame sheet shapes of soot-free methane-fueled laminar jet diffusion flames in coflowing air. From Xu et al. (2000b).

These properties are of interest because they provide well-defined parameters that can be used to highlight differences between nonbuoyant and buoyant flames and to provide ways of evaluating soot formation and oxidation models. There also is interest in laminar smoke points because allowable flame test conditions are often limited by the requirement not to emit soot. For analogous reasons, there is interest in laminar soot points due to the vastly simplified chemistry of soot-free flames which makes them much more tractable for detailed numerical simulations of flame chemistry than corresponding soot-containing flames .

A third issue of interest during this phase of the investigation involved ways to minimize soot concentrations in flames as well as soot emissions from flames by manipulating the flow environment of flames. In particular, Hussman and Maybachs (1961) demonstrated long ago that hydrocarbon-fueled diffusion flames where initial fuel velocities were retarded compared to initial air (or oxidant) velocities resulted in startling reductions of soot concentrations in flames and tendencies for soot emissions from flames. Subsequent work by Lin and Faeth (1996a,1996b,1998,2000) and Dai and Faeth (2000) also demonstrated that retarded fuel velocities compared to air (oxidant) velocities extended conditions where laminar diffusion flames did not either emit or contain soot.

In view of these observations, three issues concerning the soot and smoke-point properties of laminar jet diffusion flames were considered, as follows: state relationships for soot properties, laminar soot and smoke-point properties and hydrodynamic suppression of soot. Nonbuoyant flames were emphasized during this work because effects of buoyancy modify soot properties in flames and tend to obscure important trends. Experimental methods for the work were already described in connection with the shape properties of laminar jet diffusion flames and will not be considered again here. Finally, the following description of this work is brief, more details can be found in Dai and Faeth (2000), Faeth (1997,2001), Lin and Faeth (1996a,1996b,1998,2000) and Urban et al. (1998,2000).

State Relationships for Soot Properties. A relatively primitive level of modeling of the structure of diffusion flames is based on finding state relationships for various degrees of flame strain in order to develop laminar flamelet libraries. These libraries are then used to find the structure of turbulent diffusion flames. State relationships generally are found from measurements in laminar diffusion flames, which is quite reasonable for scalar properties such as the concentrations of major gas species and temperatures. This approach avoids current limited understanding of soot processes in flames, and for the present, provides more reliable state relationships than predictions of numerical simulations involving detailed treatment of soot chemistry. This approach is not effective for soot properties, however, because buoyancy affects soot paths differently for different parts of buoyant laminar diffusion flames (as discussed in

connection with Fig. 1) so that these properties do not exhibit the universal (path independent) behavior of properties having proper state relationships. It is the premise of this phase of the investigation that when effects of buoyancy are small, the true state relationships for soot properties within practical flames, which generally are not buoyant, can be found from observations of laminar flames.

The simplified analysis considered in the last section helps to understand flame shape properties, and can provide some justification for the presence of universal soot property state relationships, say for soot volume fractions, in nonbuoyant laminar jet diffusion flames. An important result of this simplified analysis is illustrated in Fig. 20. This involves sketches of streamlines for nonbuoyant laminar jet diffusion flames as well as the location of the flame sheet. In this flow there are two fundamental groups of streamlines: (1) internal streamlines that originate at the nozzle exit and pass directly through the flame sheet, and external streamlines that originate outside the nozzle exit and initially pass inside the flame sheet before turning and passing outside the flame sheet once again. The two groups of streamlines are separated by the "dividing streamlines" that originate from the nozzle wall itself, and are sketched in Fig. 20. As a practical matter, most of the soot generated in laminar diffusion flames is generated by soot particles passing along internal streamlines because these paths spend the most time at the fuel-rich conditions that favor the formation of soot. Now a remarkable feature of nonbuoyant laminar jet diffusion flames (achieved exactly under the approximations used in the simplified flame shape analysis and more probably just approximately for actual flames having variable physical properties, etc.) is that the variation of all scalar properties as a function of time for soot traveling along internal streamlines is identical, i.e., the variation with time is independent of the path. Given this fact, rates of soot growth and oxidation along all of these paths should be identical which implies that *all* soot properties should be identical as well. For such circumstances, soot properties as a function of the degree of mixing (represented by the fuel equivalence ratio or mixture fraction) should also be independent of the path and should exhibit universal properties as a function of, say, mixture fractions so that state relationships for soot volume fractions should be observed, similar to other scalar properties in laminar diffusion flames. Furthermore, this relationship is independent of the velocity of the fuel near the burner exit or source of the flame because doubling (say) the fuel velocity simply doubles the length of the flame between the burner exit and the flame sheet along any streamline, so that the variation of flow properties as a function of time remains unchanged. For such circumstances, the flame and soot property state relationships are independent of both the streamline path (in the region enclosed by the dividing streamlines) and the initial fuel/air (oxidant) state so that universal state relationships suitable for a broad range of flame conditions should be achieved.

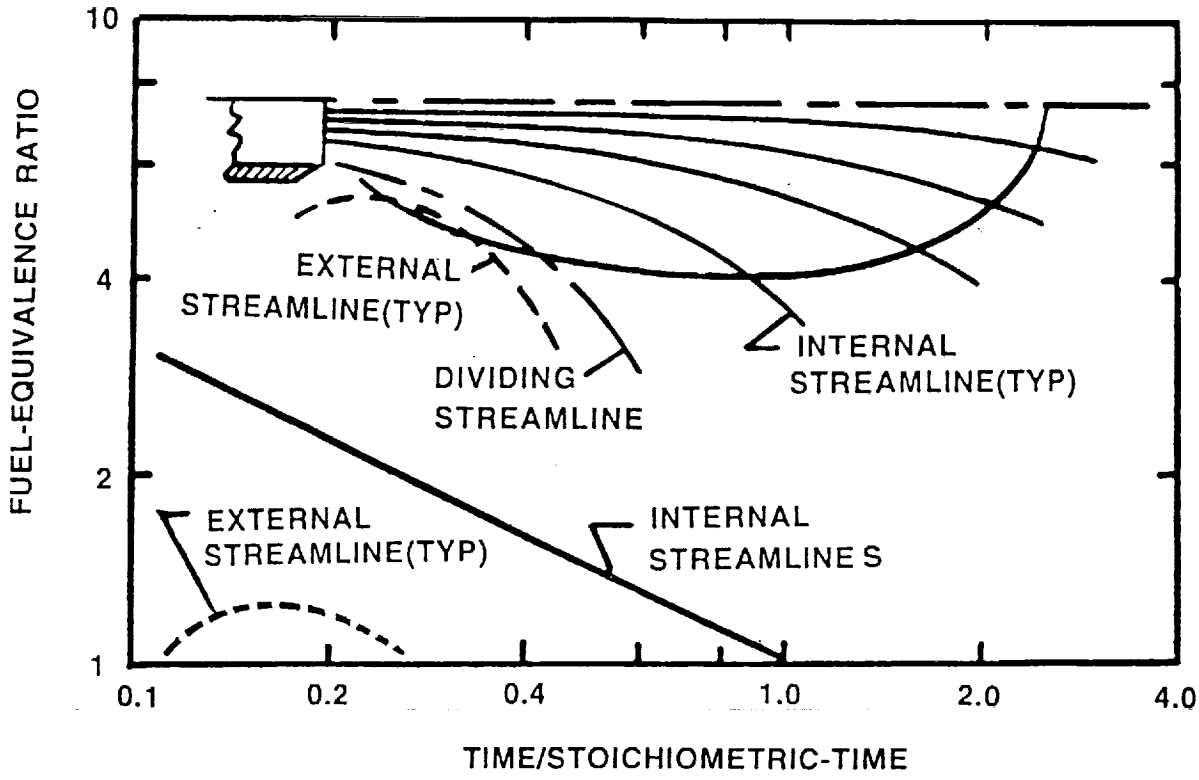

Fig. 20 Sketch of scalar property variations in nonbuoyant laminar jet diffusion flames in still air.

Measurements of both soot properties and gaseous scalar properties (sufficient to allow the local mixture fraction to be computed) in completely nonbuoyant laminar jet diffusion flames having small effects of radiation and thermophoresis are needed to convincingly evaluate laminar flamelet concepts for soot properties and to demonstrate the existence of universal state relationships for soot properties in laminar diffusion flames for given burner exit and ambient compositions, temperatures and pressures. Unfortunately, these requirements are beyond the capabilities of currently planned space-based laminar diffusion flame experiments. In particular, the LSP experiment can adequately define soot concentration and temperature properties within steady and nonbuoyant laminar jet diffusion flames but does not have the capability to measure the gaseous compositions of the test flames and thus their local mixture fractions. Nonetheless, data from the LSP experiments can provide evidence for necessary (but not sufficient) conditions for the existence of soot volume fraction state relationships in properly steady and nonbuoyant laminar jet diffusion flames when effects of radiation and thermophoresis are small. In particular, if the variation of scalar properties as a function of time are universal for streamlines within the dividing streamlines as illustrated in Fig. 20, the soot formation and oxidation amounts along each streamline should be identical which implies that maximum soot concentrations should be the same for various streamlines passing from the burner exit to the surroundings of the flame.

Measurements relating to the potential existence of soot volume fraction state relationships are illustrated in Fig. 21. These results involve crosstream distributions of soot volume fractions for an ethylene-fueled laminar jet diffusion flames burning in still air from the LSP Space Shuttle experiments (LSP Experiment 03E* as defined by Lin et al. (1999) and Urban et al. (1998,2000)). This experiment was carried out at a total pressure of 50 kPa, where effects of radiation and thermophoresis of soot particles were small due to the relatively large flow velocities within the flame sheet. Two sets of results are shown on this plot, measured early and late in the combustion process, with the latter exhibiting somewhat broader and somewhat smaller maximum concentrations due to the somewhat smaller ambient oxygen concentration caused by oxygen consumption by the flame with increasing time. In any event, it is evident that maximum soot concentrations are nearly the same at each time when data is shown in Fig. 21 (in the range 1.5-2.0 ppm) for the various paths from the burner exit to the surroundings. This behavior satisfies a necessary condition for the existence of a soot volume fraction state relationship for this flame condition. An exception to this behavior is the first streamwise position shown in Fig. 21, z=20 mm, where the maximum soot concentration (0.7 ppm) is roughly half that of the other paths. This behavior corresponds to well known exceptions to state relationships for major gas species in laminar jet diffusion flames associated with points of flame attachment. Another factor influencing soot concentrations near the burner exit is the different convection pattern of soot particles outside the dividing streamlines compared to the rest of the

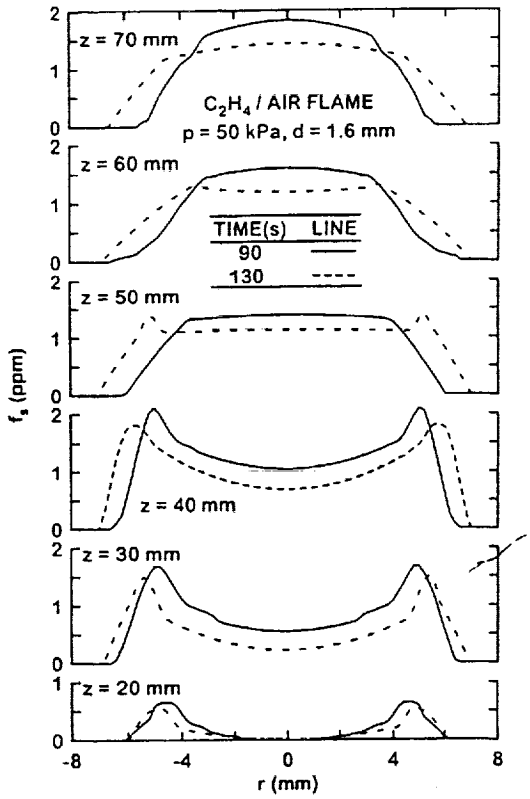

Fig. 21 Measurements of soot volume fraction distributions in a nonbuoyant laminar jet diffusion flame. From Urban et al. (1998).

flow as discussed in connection with Fig. 20. Nevertheless, the bulk of the flame is not influenced by these effects and exhibits potential for the existence of soot concentration state relationships.

Additional evidence providing necessary conditions for the existence of state relationships for soot concentration state relationships in steady and nonbuoyant laminar jet diffusion flames for conditions when effects of radiation and thermophoresis are small is provided in Fig. 22. These results were all obtained from the LSP Space Shuttle experiments (Experiment 03E*, 02E, 03E and 17E) when characteristic residence times, t_{ch} = 18-63 ms, were sufficiently small so that effects of radiation and thermophoresis were small. The paths considered, with one exception for illustrative purposes only, were generally beyond the region where effects of flame attachment and flow outside the dividing streamlines are factors. The results shown on the figure are the ratio of the maximum soot volume fraction for a path to the average of the maximum soot volume fraction for all paths considered, SVF/SVF_{avg}, plotted as a function of the ratio of the streamwise position where maximum was observed to the luminous flame length, z/L_f. Aside from one near-injector exception, the values of SVF/SVF_{avg}, are seen to all be unity with experimental uncertainties. Thus, these findings support the necessary conditions for the presence of soot volume fraction state relationships for steady and nonbuoyant laminar jet diffusion flames when effects of radiation and thermophoresis are small. More evidence along these lines will be sought during future LSP experiments where improved understanding of the properties of these flames will allow test conditions to be selected where effects of unsteadiness, buoyancy, radiation and thermophoresis that obscure observations of soot volume fraction state relationships can be avoided.

Laminar Smoke Point Properties. Laminar smoke point properties , i.e., the length of a laminar jet diffusion flame when it just begins to emit soot, were measured for round laminar jet diffusion flames in still air at various pressures. Two flame arrangements were used for these measurements of non-buoyant flames: (1) the KC-135 aircraft facility, and (2) the LSP Space Shuttle facility that was described earlier. The following discussion of the laminar smoke point measurements made with these facilities is brief, more details about the KC-135 measurements can be found in Sunderland et al. (1994), whereas more details about the LSP measurements can be found in Urban et al. (1998,2000) and Lin et al. (1998). The laminar smoke point measurements in nonbuoyant flames were also supplemented by conventional measurements in buoyant flames due to Schug et al. (1980) and Sivathanu and Faeth (1990a).

In view of the different mechanisms leading to the onset of soot emissions for buoyant and nonbuoyant laminar jet diffusion flames, it is not surprising that they have substantially different laminar smoke point properties. This behavior is illustrated in Figs. 23 and 24 by plots

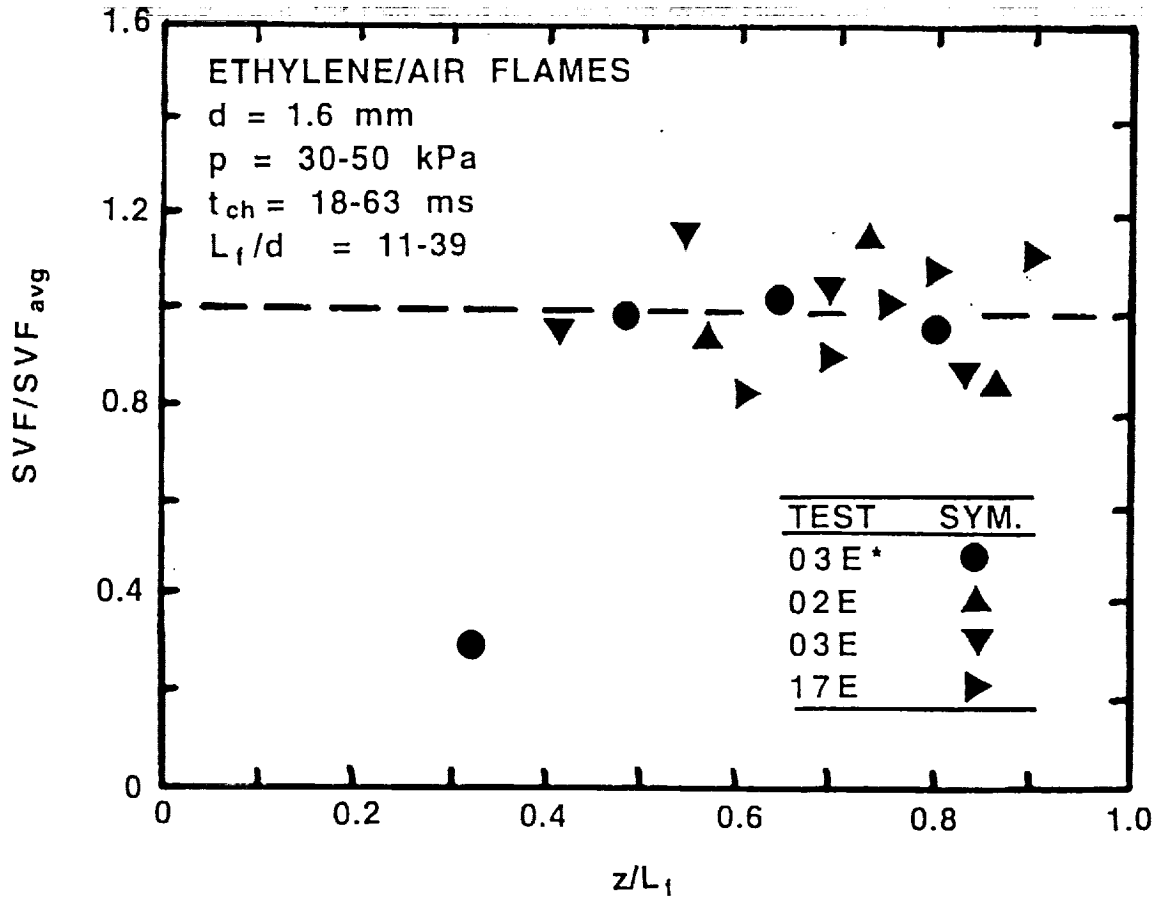

Fig. 22 Maximum soot volume fractions along internal streamlines for closed-tip non-buoyant laminar jet diffusion flames.

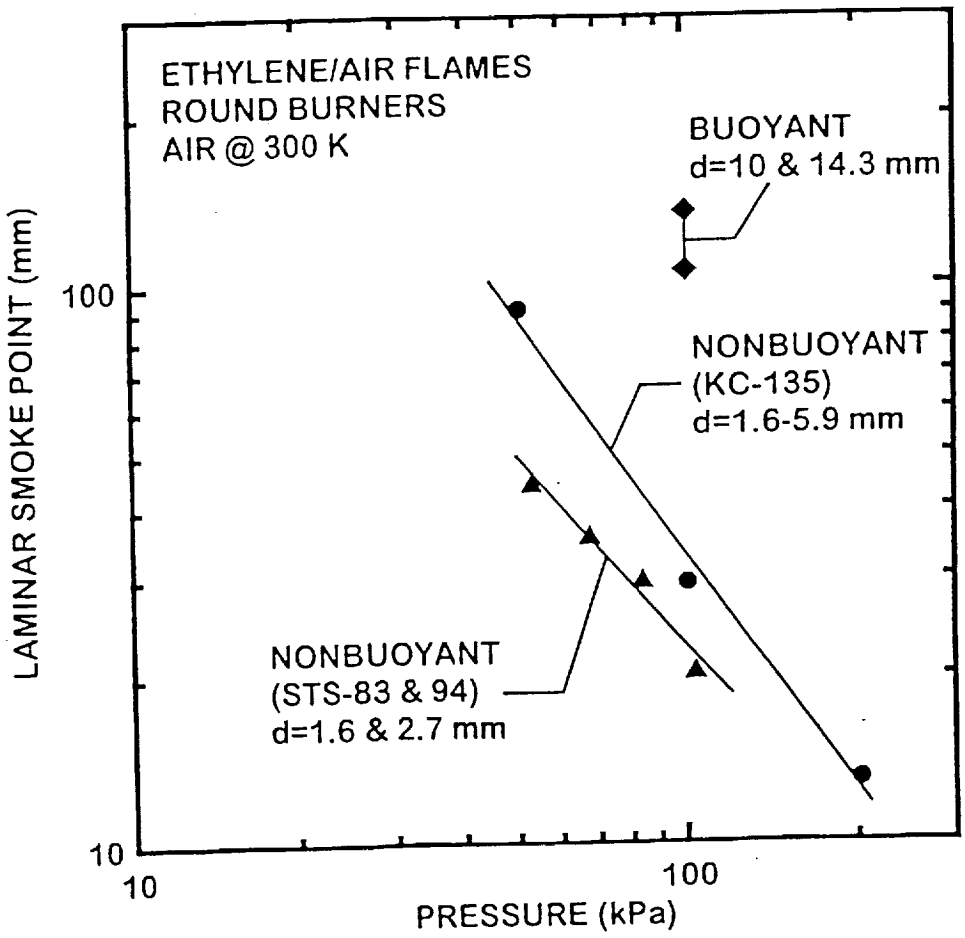

Fig. 23 Laminar smoke-point flame lengths of ethylene-fueled round non-buoyant and buoyant laminar jet diffusion flames burning in still air as a function of pressure. Non-buoyant results from Urban et al. (2000), non-buoyant KC-135 results from Sunderland et al.(1994), and buoyant results from Schug et al. (1980) and Sivathanu and Faeth (1990a). From Urban et al. (2000).

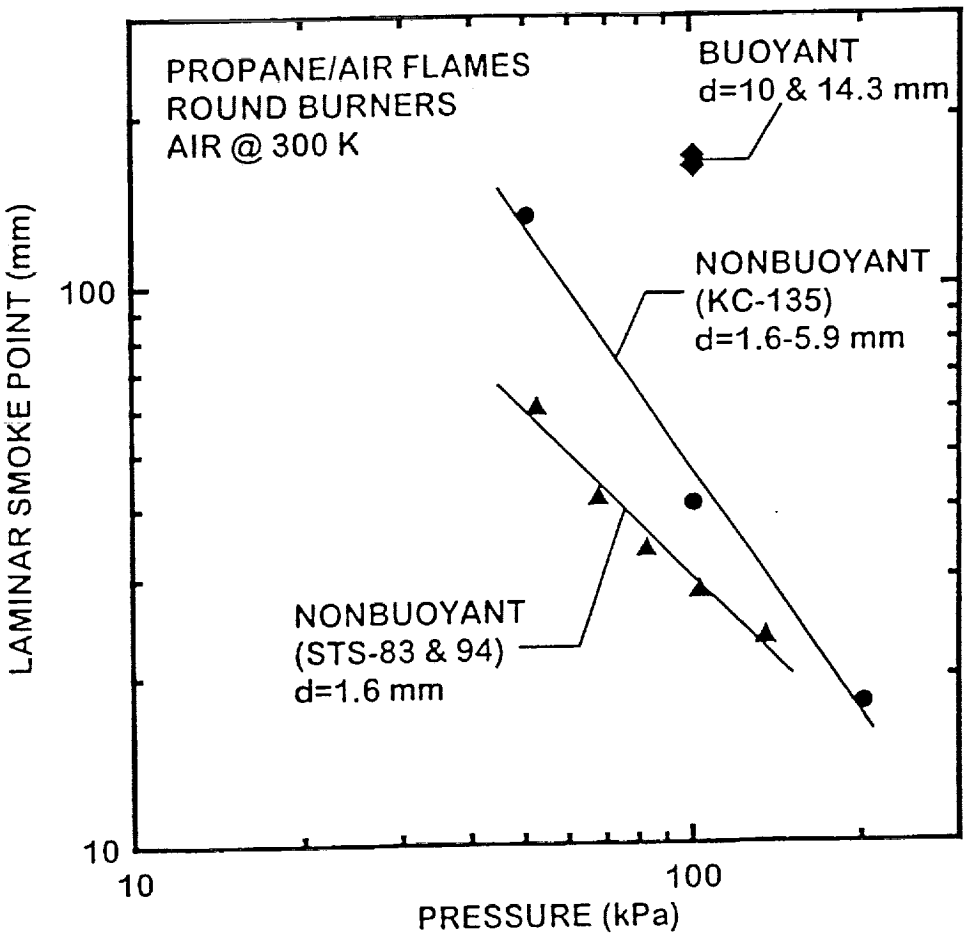

Fig. 24 Laminar smoke-point flame lengths of propane-fueled round non-buoyant and buoyant laminar jet diffusion flames burning in still air as a function of pressure. Non-buoyant results from Urban et al. (2000), non-buoyant KC-135 results from Sunderland et al. (1994) and buoyant results from Schug et al. (1980) and Sivathanu and Faeth (1990). From Urban et al. (2000).

of laminar smoke point flame lengths as a function of pressure for ethylene- and propane-fueled flames. Measurements illustrated in the figures include results for non-buoyant flames having exit diameters of 1.6 and 2.7 mm from the space-based experiments (Urban et al., 1998,2000), results for non-buoyant flames having jet exit diameters of 1.6, 2.7 and 5.6 mm from Sunderland et al. (1994) using the KC-135 low gravity facility, and results for buoyant flames having jet exit diameters of 10.0 mm from Schug et al. (1980) and 14.3 mm from Sivathanu and Faeth (1990a).

There are several interesting features about the measurements illustrated in Figs. 23 and 24. First of all, the laminar smoke point flame lengths of non-buoyant flames are significantly smaller than those of the buoyant flames. In particular, the laminar smoke point flame lengths of the ground-based non-buoyant flames up to 6.4 times longer than the space-based (STS 83 and 94) non-buoyant flames at comparable conditions. This behavior comes about because the non-buoyant flames have much larger characteristic residence times (up to 300 ms, see Lin et al. (1998)) than the buoyant flames (up to 50 ms, see Sivathanu and Faeth (1990a)), due to buoyant motion, in spite of the greater length of the buoyant flames. This provides greater potential for radiative heat losses for the nonbuoyant flames, leading to radiant quenching of soot oxidation reactions which tends to promote soot emissions.

Another important feature of the laminar smoke point flame lengths illustrated in Figs. 23 and 24 is that the space-based nonbuoyant laminar smoke point flame lengths are significantly smaller than corresponding measurements in nonbuoyant flames using ground-based (KC-135) facilities — up to a factor of 2.3 shorter at comparable conditions. This behavior is caused by the closer approach to steady, non-buoyant flame properties during the long-term space experiments compared to the relatively unsteady and disturbed microgravity environment of the KC-135 facility. In particular, flow velocities are very small near the flame tip of non-buoyant laminar jet diffusion flames and can be disturbed by small levels of g-jitter. This behavior results in enhanced mixing which delays radiative quenching. This behavior is exacerbated by the relatively slow development of non-buoyant flames for the relatively large jet exit diameters considered during the KC–135 experiments so that flame response times generally were longer than periods when the test apparatus was free of disturbances. Additional evidence of enhanced mixing during the ground-based microgravity tests compared to the space-based tests is provided by observations of generally shorter luminous flame lengths at comparable conditions for the ground-based tests than the space-based tests, as discussed in connection with Fig. 15.

Another difference between the laminar smoke point properties of non-buoyant flames from ground-based and space-based microgravity facilities involves the pressure dependence. In particular, the space-based experiments yield laminar smoke point flame lengths that are roughly inversely proportional to pressure. This effect of pressure comes about because increased

pressures tend to increase rates of soot formation and to increase residence times available for soot growth for given burner conditions and flame lengths: both of these effects imply smaller flame lengths for the onset of soot emissions as pressure increases. In contrast, the more disturbed microgravity environment of the ground-based facilities yields an even stronger effect of pressure on reducing laminar smoke point flame lengths as discussed by Urban et al. (2000).

Other properties of the laminar smoke point plotted in Figs. 23 and 24 are qualitatively similar for non-buoyant space-based flames and buoyant flames. In particular, effects of jet exit diameter on laminar smoke point flame lengths are small in all three cases and all three flame conditions indicate that ethylene-fueled flames emit soot more readily than propane-fueled flames.

Hydrodynamic Suppression of Soot. The last issue considered during this phase of the LSP investigation involved studies of hydrodynamic ways to suppress the formation of soot. As noted earlier, this work was based on the original ideas of Hussman and Maybach (1961) who demonstrated that soot formation in hydrocarbon diffusion flames was suppressed whenever initial fuel velocities were retarded compared to initial air (or oxidant) velocities. Present studies of the shapes of laminar jet diffusion flames in coflowing air, discussed in Section 4.4, help to provide an explanation of this behavior. In particular, the position of the flame sheet in laminar jet diffusion flames in strong coflow is mainly fixed by the fuel flow velocity, and as a result the characteristic residence time in the flame is inversely proportional to the air coflow velocity Lin and Faeth (1999). Thus, by retarding the fuel flow velocity, flame residence times can be made sufficiently small to prevent soot emissions from the flame or even soot formation in the flames (Lin and Faeth 1996a, Dai and Faeth, 2000). The objective of this phase of the investigation was to investigate the suppression of soot formation in laminar jet diffusion flames in coflow by retarding fuel velocities.

The test arrangement used for this study was similar to the arrangement used by Lin and Faeth (1996a,1999). Measurements were carried out at subatmospheric pressures to minimize effects of buoyancy (Law and Faeth, 1994). The test burner was a vertical coaxial tube with fuel flowing from an inner port having inside diameters of 1.7, 3.2 and 6.4 mm and air flowing from an outer port having an inside diameter of 60 mm. The burner was operated within a windowed chamber having an inside diameter and length of 300 and 1200 mm, respectively. Acetylene-, ethylene-, propane- and methane-fueled laminar jet diffusion flames in coflowing air were considered.

Lin and Faeth(1996a) had considered effects of fuel and air velocities for the soot emission of laminar coflowing jet diffusion flames, i.e., on laminar smoke point properties.

Thus, present work considers both laminar smoke-point and the laminar soot- point, i.e., the latter being the condition where flame first begins to emit soot based on observations of yellow luminosity from hot soot particles. Flame shapes were also considered during these tests as discussed earlier in Section 4.4. The following discussion of the results will be brief, for more details see Lin and Faeth(1996a) and Dai and Faeth (2000).

Some typical measurements of the fuel flow rate at the first appearance of soot emissions, the laminar smoke-point, are illustrated in Fig. 25 for 1-3 butadiene; results for other fuels are similar. As can be seen from the figure, increasing u_a/u_f, or correspondingly retarding the fuel flow velocity, clearly increases Q_f which implies larger fuel burning rates, or longer flames, prior to the emission of soot. Put another way, the flame has greater resistance to soot formation as the air/fuel velocity ratio increases. The effect of increasing u_a/u_f to increase the fuel flow rate when soot is first emitted is most evident at low pressures where effects of buoyancy are minimized and velocity ratios over the length of flames tend to change least from initial velocity ratios. The reduced effect of air/fuel velocity rate on Q_f as the pressure increases is due to effects of buoyancy because u_a/u_f is no longer representative of velocity ratios over most of the flame due to buoyant acceleration of the heated region near the flame sheet. This behavior has made it difficult to recognize the important effect of reactant stream velocity ratios on soot processes in laminar jet diffusion flames because most past observations of laminar smoke point properties have been carried out at normal gravity and atmospheric pressure (Lin and Faeth, 1996a).

Some typical measurements of laminar smoke point properties at various air coflow velocities are illustrated in Fig. 26 for propane-fueled flames; results for other fuels are similar. This is a plot of fuel flow rates at the laminar soot point as a function of the air coflow velocity for various pressures. On this plot, the reversed-shaded symbols indicate the condition where the initial air and fuel velocities are the same. These results show that increased air coflow velocities increase laminar soot point fuel flow rates. Similar to the smoke point results seen in Fig. 25, the effect of air coflow on the laminar soot point properties is best seen at low pressures where effects of buoyancy on flow velocities are minimized. It is also evident that flame liftoff tends to limit the degree to which the laminar soot point can be increased so that effective use of this technique to minimize soot formation requires ways to enhance flame attachment in the presence of large coflow velocities as well. In any event, the results illustrated in Figs. 25 and 26 clearly demonstrate the significant capabilities of retarded fuel velocities to reduce soot formation and emissions from laminar diffusion flames, as suggested long ago by Hussman and Maybach (1960). Notably, use of air atomization for combusting liquid fuel sprays involves retarded fuel velocities due to the relatively small fuel velocities and relatively large air velocities used for the atomization process. Thus, based on present results, it is not surprising that this injector system is well known to reduce soot emissions from spray flames.

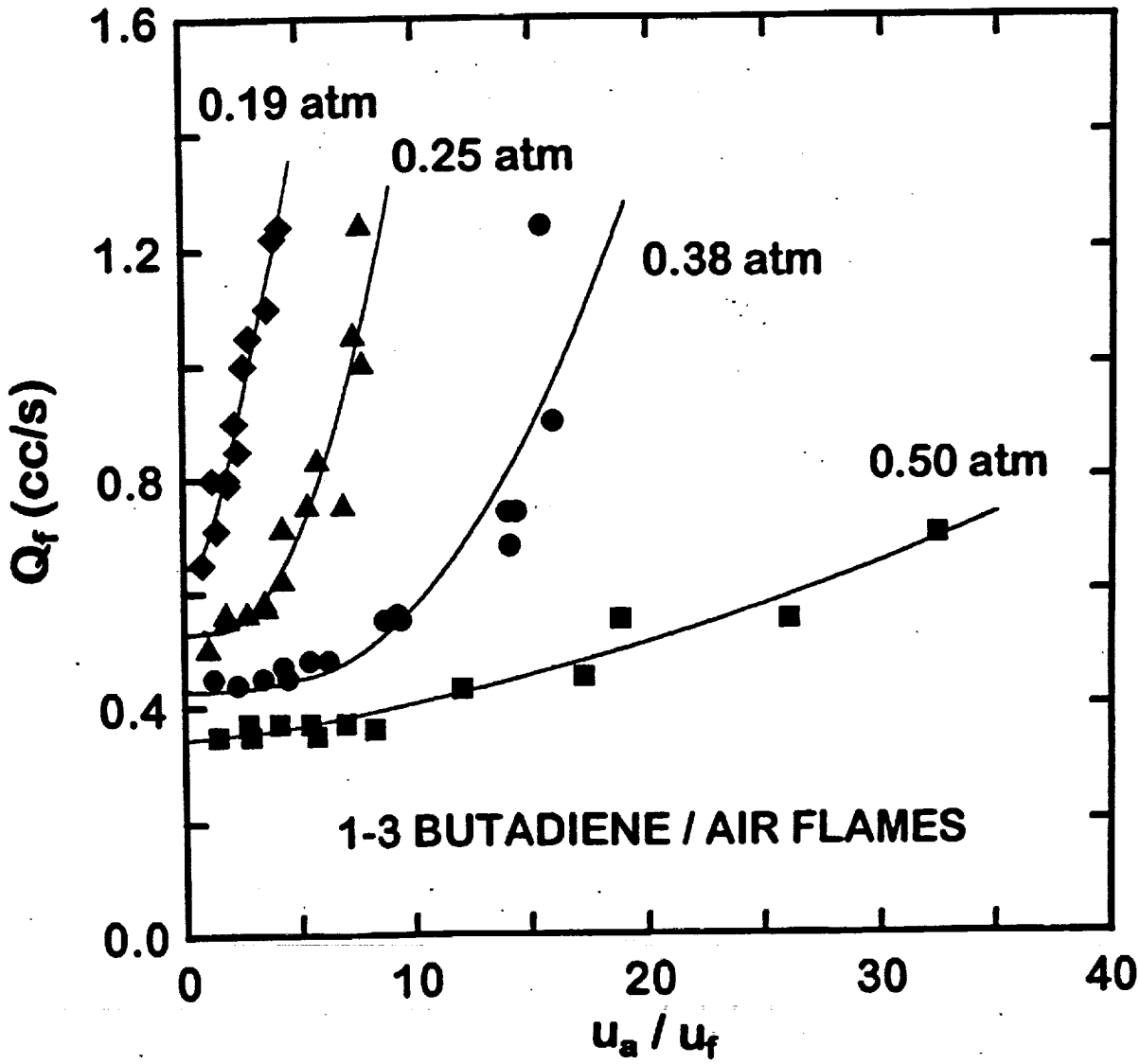

Fig. 25 Laminar smoke-point fuel flow rates for laminar jet diffusion flames fueled with 1,3-butadiene in coflowing air. From Lin and Faeth (1996a).

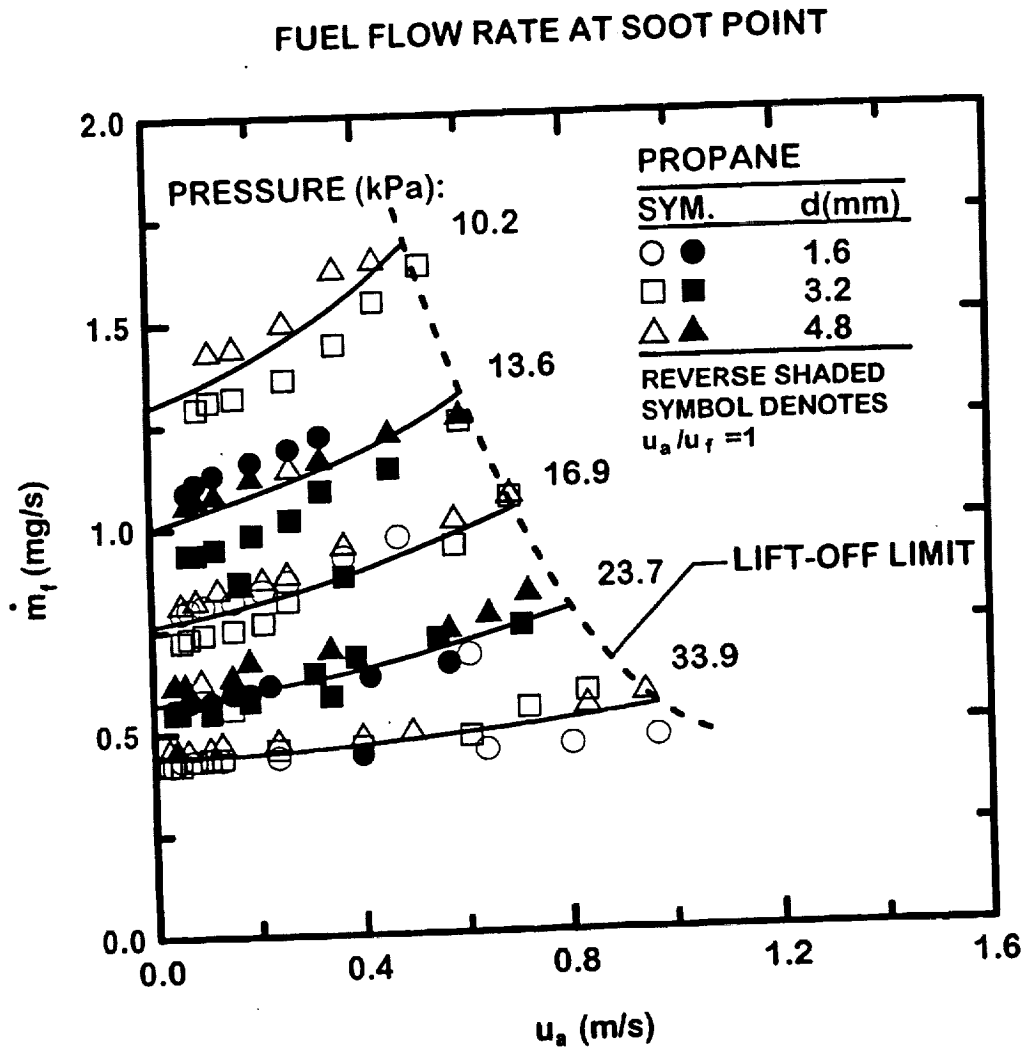

Fig. 26 Laminar soot-point fuel flow rates for laminar jet diffusion flames fueled with propane in coflowing air. From Dai and Faeth (2000).

4.6 Conclusions

Studies of the structure (shape) and soot and smoke point properties of laminar jet diffusion flames were carried out, seeking to minimize effects of buoyancy and obtain the properties of the nonbuoyant flames of greatest interest for practical applications. The main objectives of the studies were as follows: to observe flame sheet shapes for soot-free flames and to use these results to develop simplified models of these fundamental properties; to complete similar considerations for soot-containing laminar jet diffusion flames; and to consider the soot- and smoke-point properties of nonbuoyant laminar diffusion flames, e.g., to investigate whether diffusion flames exhibit state relationships for soot properties, to investigate effects of buoyancy on laminar soot- and smoke-point properties and to investigate hydrodynamic ways to control soot formation in diffusion flames. The main conclusions of the studies are as follows:

1. Soot-containing laminar jet diffusion flames had larger luminous flame lengths than earlier ground-based observations: 40% larger than luminous flame lengths using an aircraft (KC-135) facility due to reduced effects of gravitational disturbances (g-jitter), roughly twice as long as luminous flame lengths in buoyant flames at normal gravity due to the absence of effects of buoyant mixing, and roughly twice as long as luminous flame lengths in soot-free nonbuoyant flames due to soot luminosity.

2. The simplified theoretical analysis of Spalding (1976) for nonbuoyant laminar jet diffusion flames in still air yielded excellent correlations of luminous flame shapes of both soot-containing and soot-free flames upon adjusting an empirical flame length parameter to account for the fact that flame luminosity ends at the location of soot consumption and at the location of the stoichiometric flame sheet along the axis of soot-containing and soot-free flames, respectively. In fact, soot-containing flames at the laminar smoke point are roughly twice as long as the location of the flame sheet.

3. An extension of the simplified analysis of Mahalingam et al. (1990) provided reasonably good predictions of the shapes of laminar jet diffusion flames in strong coflow. Similar to the behavior of laminar jet diffusion flames in still gases, soot-containing laminar jet diffusion flames in strong coflow at the laminar smoke point were roughly twice as long as the location of the flame sheet. In addition, the laminar diffusion flames in strong coflow are 2/3 as long as corresponding flames in still gases.

4. Based on the simplified analysis of flame shapes for laminar jet diffusion flames in still gases, the environment of soot particles passing along streamlines within the dividing

streamlines of the flow causes identical variations of scalar properties as a function of time (independent of both the streamline followed and the initial velocity of the jet). This implies identical soot formation and oxidation properties, and thus soot properties, as a function of time along these paths. Such behavior suggests that universal state relationships giving soot properties as a function of the degree of mixing (or the mixture fraction) should be observed for nonbuoyant laminar jet diffusion flames (and thus in nonbuoyant turbulent jet diffusion flames based on laminar flamelet concepts). This behavior was confirmed based on tests of nonbuoyant laminar jet diffusion flames using Space Shuttle facilities which exhibited identical maximum soot concentrations for all paths from the burner exit through the flame sheet to the surroundings, which is a necessary condition for the existence of universal state relationships for soot properties.

5. Based on the simplified analysis of flame shapes of laminar jet diffusion flames in coflowing air, increased air/fuel velocity ratios for such flames should reduce residence times and thus the capability to form soot in these flames. This property was demonstrated directly by experiments that showed increased laminar smoke- and soot- point flame lengths and fuel flow rates with increasing air/fuel stream velocity ratios. These effects were most pronounced at low pressures, where effects of buoyancy were minimized, and initial air/fuel stream velocity ratios are reasonably representative of the entire visible portion of the flame for present test conditions. This effect is probably responsible for reduced sooting tendencies of liquid hydrocarbon spray flames using air atomization techniques because these methods intrinsically provide enhanced air/fuel stream velocity ratios due to the large air velocities and small fuel velocities that are used.

References

Bilger, R.W. (1976) "Turbulent Jet Diffusion Flames," *Prog. Energy Combust. Sci.* 1, 87-109.

Bockhorn, H., Fetting, F., Wannemacher, G. and Wentz, H. W. (1982) "Optical Studies of Soot Particle Growth in Hydrocarbon Oxygen Flames," *Proc. Combust. Inst.* 19, 1413-1420.

Bockhorn, H., Fetting, F., Heddrich, A. and Wannemacher, G. (1984) "Investigation of the Surface Growth of Soot in Flat Low Pressure Hydrocarbon Oxygen Flames," *Proc. Combust. Inst.* 20, 979-988.

Burke, S.P. and Schuman, T.E.W. (1927) "Diffusion Flames," *Ind. Engr. Chem.* 20, 998-1004.

Colket, M.B., and Hall, R.J. (1994) "Successes and Uncertainties in Modelling Soot Formation in Laminar Premixed Flames," *Soot Formation in Combustion* (H. Bockhorn, editor), Springer-Verlag, Berlin, pp. 442-470.

Dai, Z., and Faeth, G.M. (2000) "Hydrodynamic Suppression of Soot Formation in Laminar Coflowing Jet Diffusion Flames," *Proc. Combust. Inst.* 28, 2085-2092.

El-Leathy, A.M., Xu, F. and Faeth, G.M. (2001) "Soot Formation in Laminar Hydrocarbon/Air Diffusion Flames at Atmospheric Pressure," *Combust. Flame*, in preparation.

Faeth, G.M. (1991) "Homogeneous Premixed and Nonpremixed Flames in Microgravity: A Review," *Proceedings of the AIAA/IKI Microgravity Science Symposium—Moscow,* AIAA, Washington, pp. 281-293.

Faeth, G. M. (1997) "Combustion Fluid Dynamics (Tools and Methods)," *Proceedings of the Workshop on Fuels with Improved Fire Safety*, National Academy Press, Washington, DC, pp. 81-96.

Faeth, G.M. (2000a) "Radiation in Participating Turbulent Environments," *Appl. Mech. Rev.*, invited.

Faeth, G.M. (2000b) "Optical and Radiative Properties of Soot in Flame Environments," *Prog. Energy Combust. Sci.*, invited.

Faeth, G.M. (2001) "Gaseous Laminar and Turbulent Diffusion Flames," *Microgravity Combustion Science* (H.D. Ross, editor), Academic Press, New York, pp. 83-182.

Faeth, G. M. and Köylü, Ü.Ö. (1995) "Soot Morphology and Optical Properties in Nonpremixed Turbulent Flame Environments," *Combust. Sci. Tech.* 108, 207-229.

Faeth, G.M. and Köylü, Ü.Ö. (1996) "Structure and Optical Properties of Flame-Generated Soot," *Transport Phenomena in Combustion*, (S.H. Chen, editor), Taylor & Francis, Washington, Vol. 1, pp. 19-44.

Farias, T.L., Carvalho, M.G., Köylü, Ü.Ö. and Faeth, G.M. (1995) "Computational Evaluation of Approximate Rayleigh-Debye-Gans/Fractal-Aggregate Theory for the Absorption and Scattering Properties of Soot," *J. Heat Trans.* 117, 152-159.

Farias, T.L., Carvalho, M.G., Köylü, Ü.Ö. and Faeth, G.M. (1995) "Light Scattering from Soot Aggregates with Radially Inhomogeneous Primary Particles," *Int. J. Heat Tech.* 13, 27-47.

Farias, T.L., Carvalho, M.G., Köylü, Ü.Ö. and Faeth, G.M. (1996) "Total Scattering and Absorption Cross Sections of Carbonaceous Soot Particles," *International Symposium on Radiative Heat Transfer* (M.P. Mengüc, editor), Begell House, Inc., New York. pp. 296-318.

Frenklach, M. and Wang, H. (1990) "Detailed Modeling of Soot Particle Nucleation and Growth," *Proc. Combust. Inst.* 28, 1559-1556.

Frenklach, M. and Wang, H. (1994) "Detailed Mechanism and Modeling of Soot Particle Formation," *Soot Formation in Combustion* (H. Bockhorn, editor), Springer-Verlag, Berlin, pp. 165-192.

Gore, J.P. and Faeth, G.M. (1986) "Structure and Spectral Radiation Properties of Turbulent Ethylene/Air Diffusion Flames," *Proc.Combust. Inst.* 21, 1521-1531.

Gore, J.P. and Faeth, G.M. (1988) "Structure and Radiation Properties of Luminous Turbulent Acetylene/Air Diffusion Flames," *J. Heat Trans.* 110, 173-181.

Harris, S.J., and Weiner, A.M. (1983) "Surface Growth of Soot Particles in Premixed Ethylene/Air Flames," *Combust. Sci. Tech.* 31, 155-167.

Harris, S.J. and Weiner, A.M. (1983) "Determination of the Rate Constant for Soot Surface Growth," *Combust. Sci. Tech.* 32, 267-275.

Harris, S.J. and Weiner, A.M. (1984) "Soot Particle Growth in Premixed Toluene/Ethylene Flames," *Combust. Sci. Tech.* 38, 75-87.

Harris, S.J. and Weiner, A.M. (1984) "Some Constraints on Soot Particle Inception in Premixed Ethylene Flames," *Proc. Combust. Inst.* 20, 969-978.

Hawthorne, W.R., Weddell, D.S. and Hottel, H.C. (1949) "Mixing and Combustion in Turbulent Gas Jets," *Proc. Combust. Inst.* 3, 266-288, .

Hussman, A.W. and Maybach, G.W. (1961) "The Film Vaporizer Combustor," *SAE Trans.* 69, 563-574.

Kazakov, A. and Frenklach, M. (1998) "On the Relative Contribution of Acetylene and Aromatics to Soot Particle Surface Growth," *Combust. Flame* 112, 270-274.

Kazakov, A.,Wang, H. and Frenklach, M. (1995) "Detailed Modeling of Soot Formation in Laminar Premixed Ethylene Flames at a Pressure of 10 Bar," *Combust. Flame* 100, 111-120.

Kee, R.J., Grcar, J.F., Smooke, M.D. and Miller, J.A. (1985) "A FORTRAN Program for Modeling Steady Laminar One-Dimensional Premixed Flames," Report No. SAND85-8240, Sandia National Laboratories, Albuquerque , NM.

Kee, R.J., Dixon-Lewis, G., Warnatz, J., Coltrin, M.E. and Miller, J.A. (1986) "A FORTRAN Computer Code Package for the Evaluation of Gas-Phase, Multicomponent Transport Properties," Report No. SAND86-8246, Sandia National Laboratories, Albuquerque, NM.

Köylü, Ü.Ö. and Faeth, G.M. (1992) "Structure of Overfire Soot in Buoyant Turbulent Diffusion Flames at Long Residence Times," *Combust. Flame* 89, 140-156.

Köylü, Ü.Ö. and Faeth, G.M. (1993) "Radiative Properties of Flame-Generated Soot," *J. Heat Trans.* 115, 409-417.

Köylü, Ü.Ö. and Faeth, G.M. (1994) "Optical Properties of Overfire Soot in Buoyant Turbulent Diffusion Flames at Long Residence Times," *J. Heat Trans.* 116, 152-159.

Köylü, Ü.Ö. and Faeth, G.M. (1994) "Optical Properties of Soot in Buoyant Laminar Diffusion Flames," *J. Heat Trans.* 116, 971-979.

Köylü, Ü.Ö. and Faeth, G.M. (1996) "Spectral Extinction Coefficients of Soot Aggregates from Turbulent Diffusion Flames," *J. Heat Trans.* 118, 415-421.

Köylü, Ü.Ö., Faeth, G.M., Farias, T.L. and Carvalho, M.G. (1995) "Fractal and Projected Structure Properties of Soot Aggregates," *Combust. Flame* 100, 621-633.

Law, C.K. and Faeth, G.M. (1994) "Opportunities and Challenges of Combustion in Microgravity," *Prog. Energy Combust. Sci.* 20, 65-113.

Leung, K.M. and Lindstedt, R.P. (1995) "Detailed Kinetic Modeling of C_1-C_3 Alkane Diffusion Flames," *Combust. Flame* 102, 129-160.

Leung, K.M., Lindstedt, R.P. and Jones, W.P. (1991) "A Simplified Reaction Mechanism for Soot Formation in Nonpremixed Flames," *Combust. Flame* 87, 289-305.

Libby, P.A. and Blake, T.R. (1979) "Theoretical Study of Burning Carbon Particles," *Combust. Flame* 36, 139-169.

Libby, P.A. and Blake, T.R. (1981) "Burning Carbon Particles in the Presence of Water Vapor," *Combust. Flame* 41, 123-147.

Lin, K.-C. and Faeth, G.M. (1996a) "Hydrodynamic Suppression of Soot Emissions in Laminar Diffusion Flames," *J. Prop. Power* 12, 10-17.

Lin, K.-C. and Faeth, G.M. (1996b) "Effects of Hydrodynamics on Soot Formation in Laminar Opposed-Jet Diffusion Flames," *J. Prop. Power* 12, 691-698.

Lin, K.-C. and Faeth, G.M., (1998) "Structure of Laminar Permanently-Blue Opposed-Jet Ethylene-Fueled Diffusion Flames," *Combust. Flame* 115, 468-480.

Lin, K.-C., Faeth, G.M., Sunderland, P.B., Urban, D.L. and Yuan, Z.-G., (1999) "Shapes of Nonbuoyant Round Luminous Laminar Jet Diffusion Flames in Coflowing Air," *AIAA J.* 37, 759-765.

Lin, K.-C. and Faeth, G.M. (2000) "State Relationships of Laminar Permanently-Blue Opposed-Jet Hydrocarbon-Fueled Diffusion Flames ," *Int. J. Environ. Combust. Tech.* 1, 53-79.

Lin, K.-C., Sunderland, P.B. and Faeth, G.M. (1996) "Soot Nucleation and Growth in Acetylene/Air Laminar Coflowing Jet Diffusion Flames," *Combust. Flame* 104, 369-375.

Lin, K.-C. and Faeth, G.M. (1999) "Shapes of Nonbuoyant Round Luminous Hydrocarbon/Air Laminar Jet Diffusion Flames," *Combust. Flame* 116, 415-431

Maus, F., Schäfer, T. and Bockhorn, H. (1994) "Inception and Growth of Soot Particles in Dependence of the Surrounding Gas Phase," *Combust. Flame* 99, 697-705.

Ramer, E.R., Merklin, J.F., Sorensen, C.M. and Taylor, T.W. (1986) "Chemical and Optical Probing of Premixed Methane/Oxygen Flames," *Combust. Sci. Tech.* 48, 241-255.

Rosner, D.E., Mackowski, D.W. and Garcia-Ybarra, P. (1991) "Size- and Structure-Insensitivity of the Thermophoretic Transport of Aggregated 'Soot' Particles in Gases," *Combust. Sci. Tech.* 80, 87-101.

Schug, K.P., Manheimer-Timnat, Y., Yaccarino, P. and Glassman, I. (1980) "Sooting Behavior of Gaseous Hydrocarbon Diffusion Flames and the Influence of Additives," *Combust. Sci. Tech.* 22, 235-250.

Sivathanu, Y.R. and Faeth, G.M. (1990a) "Soot Volume Fractions in the Overfire Region of Turbulent Diffusion Flames," *Combust. Flame* 81, 133-141.

Sivathanu, Y.R. and Faeth, G.M. (1990b) "Generalized State Relationships for Scalar Properties in Nonpremixed Hydrocarbon/Air Flames," *Combust. Flame* 82, 211-230.

Spalding, D.B. (1975) *Combustion and Mass Transfer*, Pergamon, New York, p. 185.

Sunderland, P.B. and Faeth, G.M. (1996) "Soot Formation in Hydrocarbon/Air Laminar Jet Diffusion Flames," *Combust. Flame* 105, 132-146.

Sunderland, P.B., Mortazavi, S., Faeth, G.M. and Urban, D.L. (1994) "Laminar Smoke Points of Nonbuoyant Jet Diffusion Flames," *Combust. Flame* 96, 97-103.

Sunderland, P.B., Köylü, Ü.Ö. and Faeth, G.M. (1995) "Soot Formation in Weakly-Buoyant Acetylene-Fueled Laminar Jet Diffusion Flames Burning in Air," *Combust. Flame* 100, 310-322.

Urban, D.L., Yuan, Z.-G., Sunderland, P.B., Linteris, G.T., Voss, J.E., Lin, K.-C., Dai, Z., Sun, K. and Faeth, G.M. (1998) "Structure and Soot Properties of Nonbuoyant Ethylene/Air Laminar Jet Diffusion Flames,"*AIAA J.* 36, 1346-1360.

Urban, D.L., Yuan, Z.-G., Sunderland, P.B., Lin, K.-C., Dai, Z. and Faeth, G.M. (2000) "Smoke-Point Properties of Nonbuoyant Round Laminar Jet Diffusion Flames," *Proc. Combust. Inst. 28, 1965-1972.*

Wieschnowsky, U., Bockhorn, H. and Fetting, F. (1988) "Some New Observations Concerning the Mass Growth of Soot in Premixed Hydrocarbon/Oxygen Flames," *Proc. Combust. Inst.* 22, 343-352.

Xu, F. and Faeth, G.M. (2000) "Structure of the Soot Growth Region of Laminar Premixed Methane/Oxygen Flames," *Combust. Flame* 121, 640-650

Xu, F. and Faeth, G.M. (2001) "Soot Formation in Laminar Acetylene/Air Diffusion Flames at Atmospheric Pressure," *Combust. Flame* 125, 804-819.

Xu, F., Sunderland, P.B. and Faeth, G.M. (1997) "Soot Formation in Laminar Premixed Methane/Oxygen Flames at Atmospheric Pressure," *Combust. Flame* 108, 471-493.

Xu, F., Lin, K.-C. and Faeth, G.M. (1998) "Soot Formation in Laminar Premixed Methane/Oxygen Flames at Atmospheric Pressure," *Combust. Flame* 115, 195-209.

Xu, F., El-Leathy, A.M., and Faeth, G.M. (2000a) "Soot Oxidation in Laminar Hydrocarbon/Air Diffusion Flames at Atmospheric Pressure," *Combust. Flame*, submitted.

Xu, F., Dai, Z. and Faeth, G.M. (2000b) "Flame Shapes of Nonbuoyant Laminar Jet Diffusion Flames," *AIAA J.*, submitted.